

A trace-gas climatology above Zotino, central Siberia

By JON LLOYD^{1*}, RAY L. LANGENFELDS², ROGER J. FRANCEY², MANUEL GLOOR¹, NADEJDA M. TCHEBAKOVA³, DANIIL ZOLOTOUKHINE³, WILLI A. BRAND¹, ROLAND A. WERNER¹, ARMIN JORDAN¹, COLIN A. ALLISON², VITALY ZRAZHEWSKE³, OLGA SHIBISTOVA³ and E.-D. SCHULZE¹,
¹Max Planck Institute for Biogeochemistry, Postfach 100164, 07743, Jena, Germany; ²CSIRO Atmospheric Research, Private Bag 1, Aspendale, Victoria 3195, Australia; ³Sukachev Institute of Forest, Siberian Branch, Russian Academy of Sciences, Akademgorodok, 660036 Krasnoyarsk, Russia

(Manuscript received 9 July 2001; in final form 19 June 2002)

ABSTRACT

Using light aircraft and at intervals of approximately 14 days, vertical profiles of temperature, humidity, CO₂ concentration and ¹³C/¹²C and ¹⁸O/¹⁶O ratio, as well as concentrations of CH₄, CO, H₂ and N₂O, from about 80 to 3000 m above ground level have been determined for the atmosphere above a flux measurement tower located near the village of Zotino in central Siberia (60°45'N, 89°23'E). As well as being determined from flask measurements (typically at heights of 100, 500, 1000, 1500, 2000, 2500 and 3000 m) continuous CO₂ concentration profiles at 1 Hz have also been obtained using an infrared gas analyser. This measurement program is ongoing and has been in existence since July 1998. Data to November 2000 are presented and show a seasonal cycle for CO₂ concentration of about 25 μmol mol⁻¹ within the atmospheric boundary layer (ABL) and about 15 μmol mol⁻¹ in the free troposphere. Marked seasonal cycles in the isotopic compositions of CO₂ are also observed, with that of oxygen-18 in CO₂ being unusual: always being depleted in the ABL with respect to the free troposphere above. This is irrespective of whether the CO₂ concentration is higher or lower in the free troposphere. We interpret this as indicating a net negative discrimination being associated with the net terrestrial carbon exchange, irrespective of whether photosynthesis or respiration dominates the net carbon flux in this region. During winter flights, large fluctuations in CO₂ concentration with height are often observed both within and above the stable ABL. Usually (but not always) these variations in CO₂ concentrations are associated with more or less stoichiometrically constant variations in CO and CH₄ concentrations. We interpret this as reflecting the frequent transport of polluted air from Europe with very little vertical mixing having occurred, despite the large horizontal distances traversed. This notion is supported by back-trajectory analyses. Vertical profiles of CO₂ concentration with supplementary flask measurements allow more information on the structure and composition of an air mass to be obtained than is the case for flask measurements or for ground-based measurements only. In particular, our data question the notion that there is usually anything like “well mixed background air” in the mid-to-high northern latitudes during the winter months.

1. Introduction

It is now generally accepted that land ecosystems are absorbing a significant fraction of fossil fuel CO₂ emissions and CO₂ released from the terrestrial bio-

sphere as a consequence of land-use change. However, the precise mechanisms involved and the geographical location of the terrestrial carbon sink is still uncertain (Lloyd, 1999). Although several lines of evidence point to a significant tropical sink for anthropogenic CO₂ (Grace et al., 1995; Phillips et al., 1998), many atmospheric inversion studies have also pointed towards a substantial northern hemisphere terrestrial sink (Tans et al., 1990; Ciais et al., 1995; Rayner et al., 1999; Fan

*Corresponding author.
e-mail: jon.lloyd@bgc-jena.mpg.de

et al., 1999; Kaminski et al., 1999; Ciais et al., 2000). Even so, there is still great uncertainty as to how this supposed sink is distributed across the northern continents. Fan et al. (1999) claimed that the conterminous USA constituted by far the most substantial component, whereas the inversion study of Ciais et al. (2000) found that Siberia constituted over 60% of their estimated northern hemisphere sink. A similar result was also found by Kaminski et al. (1999), who attributed about 70% of the northern hemisphere terrestrial sink in the early 1980s to the former USSR. In contrast to this, Rayner et al. (1999) concluded a much smaller northern sink overall than other atmospheric inversion studies, with the Siberian landmass being more or less carbon neutral.

It is not clear how much the selection of different periods and different averaging contributes to the apparent conflicts. In any case, the above estimates of the terrestrial carbon sink for individual regions have been quoted with significant uncertainties, a consequence of the atmospheric inverse problems being notoriously underdetermined (Enting, 1993). This is particularly the case when it comes to deducing net terrestrial fluxes. The current global CO₂ measurement network (Conway et al., 1994) is heavily biased towards oceanic sites. Although such a network may provide an optimum approach for the determination of long-term trends in CO₂ concentrations, it has been suggested that increased measurements of CO₂ concentrations over the land, and in particular regular measurements of the altitudinal variation in CO₂ concentrations, should serve to help to reduce uncertainties in net terrestrial carbon fluxes (Tans et al., 1996). This has recently been verified quantitatively by Gloor et al. (2000).

Of the northern land masses, Eurasia is by far the largest, and it is here that regular measurements of the vertical structure of CO₂ concentrations should be of the greatest benefit in verifying the existence of a significant northern hemisphere terrestrial sink and in helping pin down its geographic distribution. However, to date there has only been one report of the vertical structure of CO₂, its isotopes and other trace gases over Russia, that being the study of Nakazawa et al. (1997). The importance of an improved long-term CO₂ data set over this large landmass in constraining the results of atmospheric transport inversions can also be seen from the model intercomparison study, TRANSCOM 1, summarised by Rayner and Law (1995) and Law et al. (1996). With the same gridded monthly mean terrestrial surface exchange input

(Fung et al., 1983), all ten atmospheric transport models used were in close agreement with regard to the amplitude of the seasonal cycle at most oceanic monitoring sites. However, over central Siberia differences between models were much more profound, with the modelled amplitude ranging from only about 30 ppm to as much as 127 ppm (Rayner and Law, 1995).

A further role of Siberia in the global carbon cycle may be as a high northern terrestrial ecosystem influencing the $\delta^{18}\text{O}$ composition of atmospheric CO₂. It has been suggested that the exchange of CO₂ with isotopically depleted chloroplast water in colder regions such as Siberia gives rise to a negative ^{18}O discrimination during photosynthesis in this region (Farquhar et al., 1993). This, in conjunction with a depletion of atmospheric $\delta^{18}\text{O}$ in CO₂ by ecosystem respiration in such regions, is thought to give rise to the large observed latitudinal variation in the $\delta^{18}\text{O}$ of CO₂ (Francey and Tans, 1987; Peylin et al., 1999).

In what follows, we describe the results from the first two-and-a-bit years of aircraft flights sampling the trace gas composition of the atmosphere to a height of 3 km near the village of Zotino in central Siberia (60°44'N, 89°09'E). As well as reporting on seasonal variations in the vertical structure of the concentration and isotopic composition of CO₂, concentration data for CO, CH₄ and H₂ are also presented. A consideration of CO and/or CH₄ concentrations in conjunction with CO₂ concentration measurements can provide useful information about the origins of CO₂ variations observed, particularly the presence of pollution events (Conway et al., 1993; Harris et al., 2000). For molecular hydrogen, the large northern hemisphere land mass is considered to be the major sink (Novelli et al., 1999), with the rate of H₂ uptake by soils being biologically mediated and linked to the respiratory capacity of micro-organisms within the soil (Godde et al., 2000). Although the effects of major sources of H₂ to the troposphere such as methane oxidation (Crutzen, 1991) and biomass burning (Crutzen and Andreae, 1990) may also need to be taken into account, H₂ does, however, have the potential to be used as a tracer for the CO₂ in the atmosphere associated with soil respiratory activity.

2. Material and methods

Measurements were made near the joint Max Planck Institute for Biogeochemistry (Jena) and Institute of Forest (Krasnoyarsk) field facility, about 600 km north

of the city of Krasnoyarsk. The surrounding area consists of predominantly *Pinus sylvestris* forests interspaced with bogs; near the village of Zotino in central Siberia (60°44' N, 89°09' E). The *P. sylvestris*/bog mosaic dominates a large region of predominantly flat Western Siberian lowland extending from the Ural Mountains to the Yenisei River across a 10° latitudinal band. Much of the study area, located 30–60 km inland from the Yenisei River, has not been subject to significant human disturbance in the past and certainly not before 1942, although some areas close to villages located on the west side of the Yenisei river have been subject to extensive logging over the last 40 yr or so. A general description of the pristine pine stands typical of much of the area can be found in Wirth et al. (1999). The area is remote. Apart from Krasnoyarsk (population 900 000) and other cities along the Trans-Siberian railroad which runs about 600 km to the south of the measurement site, the nearest cities are Surgut (population 260 000) which is located about 1000 km to the west and Yakutsk (population 200 000) over 2000 km to the east. About 1000 km to the north, located on the east side of the Yenisei River, is an industrial area centered on a large nickel smelter near Norilsk. A general description of the region can be found in Schulze et al. (2002).

With an intended frequency of about every 14 days, a local Antonov-AN2 bi-plane was employed for atmospheric measurements, usually flying out of the village of Yeniseisk, about 300 km south of the measurement site. The plane was instrumented with a simple system for the analysis of the concentrations of various gases in the atmosphere as well as for the measurement of ambient temperature and pressure. Two air inlet lines of decarbon tubing were placed towards the tip of the port wings of the aircraft attached onto the outermost strut connecting the upper and lower wing sections. In this position it was considered that the chances of contamination from the 1000 hp radial plane engine exhaust (located behind the engine on the starboard side) were minimal. Both lines were about 10 m in length.

2.1. Flask sampling and analyses

One line allowed air samples to be taken for subsequent analyses at CSIRO Atmospheric Research's Global Atmospheric Sampling Laboratory (GASLAB; Francey et al. 1996) and/or a newly commissioned facility at the Max Planck Institute for Biogeochemistry in Jena, Germany. Whole air samples, pre-dried

by passage through anhydrous magnesium perchlorate at ambient atmospheric pressure, were collected in 1.0 dm³ Pyrex glass cylindrical flasks with Teflon (PFA) O-ring valves at each end (Glass Expansion P/L, Melbourne, Australia).

Flasks were filled using a pump unit specifically packaged for sampling from aircraft (Ramonet et al., 2002). Sampling involved flushing a flask for >5 min at 4 dm³ min⁻¹ at ambient pressure, then, over 10–20 s, pressurising the flask to 80 kPa above ambient (determined by a pressure relief valve), prior to closing the flask taps. Normal high-precision gas sampling procedures were implemented, including careful selection and pre-treatment of all surfaces in contact with sample air and the permanent exclusion of water vapour from flasks.

Flasks filled between July 1998 and June 2000 were analysed by CSIRO Atmospheric Research (CAR) in Aspendale, Australia. Flasks collected from July 2000 onwards were analysed in a newly commissioned facility at the Max Planck Institute for Biogeochemistry (MPI-BGC) in Jena, Germany.

CAR analyses. Samples were analysed for mixing ratios of CO₂, CH₄, H₂, CO and N₂O by gas chromatography and the isotopic ratios ¹³C/¹²C and ¹⁸O/¹⁶O in CO₂ by isotope ratio mass spectrometry. Details of instrumentation, analytical techniques and calibration are provided elsewhere (Francey et al., 1996; Allison and Francey, 1999; Langenfelds et al., 2001 and references therein). Briefly, CO₂ and CH₄ are measured using a Carle (S Series) instrument with flame ionisation detector (FID), where CO₂ is methanised on a heated nickel catalyst before detection. H₂ and CO are measured on a trace analytical reduction gas analyser, where heated mercuric oxide is reduced to mercury vapour allowing detection by UV absorption. Isotopic analyses involve a Finnigan MAT252 mass spectrometer with a modified MT Box-C trapping accessory for the cryogenic extraction of CO₂. Isotopic data are reported using the VPDB-CO₂ scale, CO₂ in the WMO mole fraction scale (relative to dry air) and CH₄ in the CSIRO94 CH₄ scale, which is derived from and remains almost identical to the CH₄ scale maintained at the National Ocean and Atmospheric Administration's Climate Monitoring and Diagnostics Laboratory (NOAA/CMDL). CO is also linked to the scale of NOAA/CMDL using a single high-pressure cylinder standard that was calibrated at NOAA/CMDL in 1992 and assigned a value of 196 ppb. However, intercomparisons between CSIRO and NOAA/CMDL show significant inter-laboratory

differences at lower mixing ratios (Masarie et al., 2001). Integrity of relative CO mixing ratios in the CSIRO data is supported by careful characterisation of instrument response functions and long-term monitoring of about 20 high-pressure cylinder standards spanning a CO range of 20–400 ppb. H₂ data are reported in the CSIRO94 H₂ scale that was established at CSIRO by “bootstrapping” to a gravimetrically derived CH₄ scale. Measurements of N₂O from Zotino samples are not reported here but are used to correct for isobaric interference with CO₂ isotopic measurements.

MPI-BGC analyses. Samples were first analysed for mixing ratios of CO₂, CH₄ and N₂O using gas chromatography, with ¹³C/¹²C and ¹⁸O/¹⁶O in CO₂ subsequently determined using an automated cryogenic extraction/isotope ratio mass spectrometry unit. Details of the instrumentation, experimental procedures and the calibration are described in detail elsewhere (Jordan and Brand, 2001; Werner et al., 2001) and are summarised only briefly here.

For concentration analysis, sample gas was flushed through two temperature-controlled sample loops of a gas chromatograph (Hewlett Packard 6890), allowed to equilibrate to ambient pressure and injected for separation onto two twin-column separation lines. CH₄ was quantified via a flame ionisation detector (FID) with CO₂ analysed on the same line after conversion to CH₄ in a methaniser unit located between the main column and the detector. N₂O was separated from other air constituents in a parallel pre- and main column line and detected on an ECD (electron capture detector). The trace gas concentration of unknown samples was inferred from intermittent measurement of a precisely calibrated reference air. Long term precision was controlled by routinely measuring a quality control standard air. For CO₂, the analytical precision was <0.1 ppm; CH₄ was determined with <2 ppb and N₂O with <0.3 ppb uncertainty per sample.

For isotopic analysis, a customised CO₂ extraction unit (BGC-AirTrap) was connected directly to an isotope ratio mass spectrometer (MAT 252, Finnigan MAT, Bremen, Germany). Gas samples were connected via 1/2" Cajon[®] Ultratorr adapters to a 16-port multiport valve (VICI/Valco, Switzerland). The trapping line has a water trap (dry ice/ethanol) and a CO₂ trap at –196 °C connected in series. CO₂ gas was measured directly from the volume of the corresponding trap via a capillary to the changeover valve of the mass spectrometer. About 600 mL of sample air was consumed. A correction for the contribution of N₂O

to the ion currents of CO₂ was applied in form of a mass balance calculation using the measured concentrations of CO₂ and N₂O in the sample and reference air. For subjecting sample air and reference air to exactly the same conditions during analysis (Werner and Brand, 2001) three positions of the multiport valve were reserved for permanently attached reference air, leaving 13 positions available for samples. A complete sequence involved two reference air measurements at the start followed by the samples and a QA standard attached to position 8. After all samples were analysed, two more reference air aliquots were then processed. Concluding from the daily analyses of the QA standard a precision performance of 0.012‰ for δ¹³C and 0.019‰ for δ¹⁸O was achieved over a period of 9 month operation (Werner et al., 2001).

Transfer of analysis responsibility from CAR to MPI-BGC. In order ensure the integrity of the time series, both laboratories worked on identical scales for mixing ratio and isotope ratio analysis. To achieve this, a set of six reference air tanks was prepared by CAR and calibrated repeatedly over a period of 2 months to provide preliminary verification of trace gas stability. Concentration ranges in those cylinders were selected to span the range of values likely to be encountered in atmospheric field sampling activities. Reference air from one of these tanks (δ¹³C = –8.078 ± 0.017‰ and δ¹⁸O = –0.847 ± 0.033‰ on the VPDB-CO₂ scale) was then utilised at MPI-BGC to establish the respective scales by routinely processing aliquots through respective sample lines between flask sample measurements.

At the time of writing, intercomparison of analytical results for flask samples between the two laboratories had been made for 170 Siberian flasks over a broad range of concentrations spanning a period of about one year. For the mixing ratios, mean deviations between CAR and MPI-BGC were very small: 0.2 ppb for CH₄ (std. dev. 1.8 ppb), –0.04 ppm for CO₂ (std. dev. 0.24 ppm), and –0.06 ppb (std. dev. 0.3 ppb) for N₂O, virtually independent of the concentration. Comparison of flasks for isotope ratio analysis was hampered by the fact that often a large amount of air had already been consumed by the various tests at CAR and MPI-BGC before isotopic analysis. A relatively large amount (600 mL) of gas is required for measurement in Jena. The limited number of analyses made confirmed that flask comparisons are not as precise as tank comparisons, mainly due to residual moisture and other flask specific effects. The average of seven direct flask comparisons was –0.001‰ for δ¹³C (std. dev.

0.045‰) and $-0.014‰$ for $\delta^{18}\text{O}$ (std. dev. 0.133‰). Within the limits of flask pair agreement, results between MPI-BGC and CAR were identical so that, as for the concentration measurements, the isotope record presented here is independent of the laboratory where the samples were analysed.

2.2. CO_2 , water vapour and temperature profiles

The second inlet line was for continuous analysis of CO_2 and concentrations using a LICOR 6251 infrared gas analyser. Air flow through the analyser was at a rate of $1.5 \text{ dm}^{-3} \text{ min}^{-1}$. The pressure of the IRGA cell was continuously monitored using a Vaisala PTB 100A pressure transmitter connected via a polyurethane tube to the output port of the sample cell. The analogue Vaisala output was passed back to the LICOR 6251 for pressure corrections according to the customised software. The LICOR pressure corrected CO_2 mole fractions and the raw barometer output were logged at 1 Hz frequency with a DELTA-T 3000 datalogger/laptop computer combination. Previous comparisons of IRGA measurements with flask data have suggested that the customised LICOR software does not fully account for pressure and temperature effects on the raw signal, with a typical overestimation at 3000 m height being about $3 \mu\text{mol mol}^{-1}$ for CO_2 (Lloyd et al., 2001a). The IRGA was therefore recalibrated regularly during each flight, typically at every 500 m elevation increment using span gases of approximately 340 and $380 \mu\text{mol mol}^{-1}$.

Also connected to the data logger with a 1 Hz acquisition time was instrumentation to measure humidity and temperature (model HMP35D, Vaisala, Helsinki, Finland), mounted on the port wing close to the gas inlet tubes (directly in the airstream) and a second barometer giving the cabin pressure.

2.3. Flight protocols

With the exception of the first two flights, for which flasks were filled at only 2000, 2500 and 3000 m height, similar protocols were employed for all flights, with the first single flask being filled at about 80 m above the tree tops and subsequent single flasks being filled at 500, 1000 and 1500 m height. At 2000, 2500 and 3000 m height duplicate flasks were filled. Flushing and filling each flask took between 6 and 7 min, with the plane circling at constant altitude during this time. Usually the IRGA calibration was also checked

using the span gases immediately upon attainment of the desired height for the filling of flasks. Flights were typically conducted around solar noon or later in the afternoon.

Generally speaking, flights were only undertaken under fair weather conditions, which for this region are generally associated with westerly or northerly air-flow. Back-trajectories at 2500 m for all flights here are given in Levin et al. (2002).

2.4. Calculation of continuous profiles

Continuous-profile data were reprocessed off-line to take into account the inability of the IRGA software to account completely for changes in atmospheric pressure on the raw output signal. This is presumably due to effects such as band broadening with the changes in pressure which occur in addition to changes in the density of CO_2 molecules in the sample cell. To achieve this, calibration gas values were interpolated between each recalibration measurement (usually every 500 m; see above) using atmospheric pressure as the independent variable. The “corrected” IRGA output (in $\mu\text{mol mol}^{-1}$) was then adjusted to reflect the “drift” in the apparent values of the calibration gases. When this was done, however, there was often still a small difference (always $<1 \mu\text{mol mol}^{-1}$ and usually $<0.5 \mu\text{mol mol}^{-1}$) between the CO_2 mole fractions as estimated by the IRGA and that obtained from flask measurements. This offset, taken to be invariant with height, has been compensated for in Figs. 1 and 2, with the profile as determined from the IRGA measurements overlain upon the flask data to provide the maximum amount of information possible about the vertical structure of the CO_2 concentration in the lower troposphere.

2.5. Trajectory analysis

The HYSPLIT4 model (Draxler and Hess, 1998) was used to calculate back trajectories of air masses sampled during measurement flights using the procedure outlined in Gloor et al. (2001).

3. Results

For the period reported on here, 7 July 1998 to 3 November 2000, 47 flights had been undertaken on a more or less bi-weekly schedule, the only significant exception being the period 25 September 1998 to

13 January 1999, when only one flight (12 November 1998) was possible due to problems with aeronautical and scientific instrumentation. In what follows, we first present representative profiles for spring/summer and autumn/winter, after which a consideration of underlying relationships between the various trace gases/isotopes and the nature of the overall seasonal cycles is examined.

3.1. Spring/Summer profiles

Four profiles, representative of those typically observed in the period from late spring to late summer (mid-March to early September) are shown in Fig. 1. As can be seen from the profile of virtual potential temperature with height (Fig. 1a) these four days (29 April, 2000, 29 May 2000, 14 June 2000 and 30 June 2000) were all characterised by a convective boundary layer (CBL) between 2 and 2.5 km depth. The CBL top is also discernible from the water vapour profiles (Fig. 1b) where marked reductions in vapour concentration occur, especially for 14 June 2000 (black line). Within the boundary layer, all four profiles were characterised by relatively constant CO₂ concentrations (Fig. 1c). In late spring (29 April 2000; red line) the concentration within the boundary layer was greater than the free troposphere above, whereas for 29 May (green line) there was very little gradient observed. For the later two flights shown here, CBL CO₂ concentrations were then noticeably lower than the free troposphere. Noteworthy is the variation in CO₂ concentration observed above the CBL on 14 June, which was also mirrored in the free troposphere water vapour profile (Fig. 1b). With the exception of the 3000 m value for 29 May, agreement between the profile structure as deduced from the IRGA output and the flask CO₂ concentration was excellent.

Summer CO concentrations were highly variable from flight to flight, and did not show any systematic vertical structure or covariance with other trace gases (Fig. 1d). For the 29 April and 29 May flights concentrations were more or less constant with height, but for the other two flights substantial variations were observed, especially above 2 km height.

Vertical profiles of $\delta^{13}\text{CO}_2$ are shown in Fig. 1e. Generally these mirrored those observed for CO₂ concentrations, with values within the CBL being depleted compared to the free troposphere above for the 29 April flight, more or less constant for 29 May and enriched with respect to the free troposphere for 14 and 30 June. Variations in the $\delta^{18}\text{O}$ of CO₂ with height were less sys-

tematic, but irrespective of the shape of the CO₂ concentration profile, tended to be more depleted within the CBL than the free troposphere above (Fig. 1f).

CH₄ concentrations are shown in Fig. 1g. This shows a large accumulation of CH₄ in the CBL for the flights of 29 April and 14 June, less accumulation for 30 June and a more or less neutral profile for 29 May.

Figure 1h shows the vertical structure of molecular hydrogen concentrations. For all four flights concentrations were reduced within the CBL as compared to the free troposphere above.

3.2. Autumn/Winter profiles

Three profiles, indicative of the typical variability observed during late autumn and winter/early spring, are shown in Fig. 2 (28 November 1999, 26 January 2000 and 4 March 2000). Profiles of virtual potential temperature (Fig. 2a) show the atmosphere to have been stably stratified on 28 November (blue line) and 4 March (black line) but, somewhat surprisingly, a constant virtual potential temperature with height to about 600 m on 26 January (red line) indicating the likely presence of a CBL. Compared to summer, water vapour concentrations were very low, relatively variable and not obviously correlated with any of the other entities examined (Fig. 2b).

Observed CO₂ concentrations varied substantially between flights. For 28 November, the CO₂ concentration at 100 m height was 383 $\mu\text{mol mol}^{-1}$, above which it declined sharply to a more or less uniform value of 369 from 300 m to 3000 m. A substantially different pattern can be seen for 26 January, where maximum concentrations as high as 385 $\mu\text{mol mol}^{-1}$ were observed around 1 km height, with a relatively sharp decline to 2 km above that height and slightly lower CO₂ concentrations below. The profile for 4 March showed a slight decline in CO₂ concentration with height to about 1 km, after which large fluctuations of as much as 4 $\mu\text{mol mol}^{-1}$ over heights as little as 100 m were observed. However, for this flight, as well as all others, once the small offset between the IRGA profile and flask values was taken into account, agreement at flask measuring heights was excellent, giving us confidence that the erratic shape of the 4 March profile is not a measurement artefact.

For the 26 January flight, CO ratios showed a structure that was very similar to that observed for CO₂, also showing maximum values around 1.2 km height (Fig. 2d). Likewise for 4 March, close examination

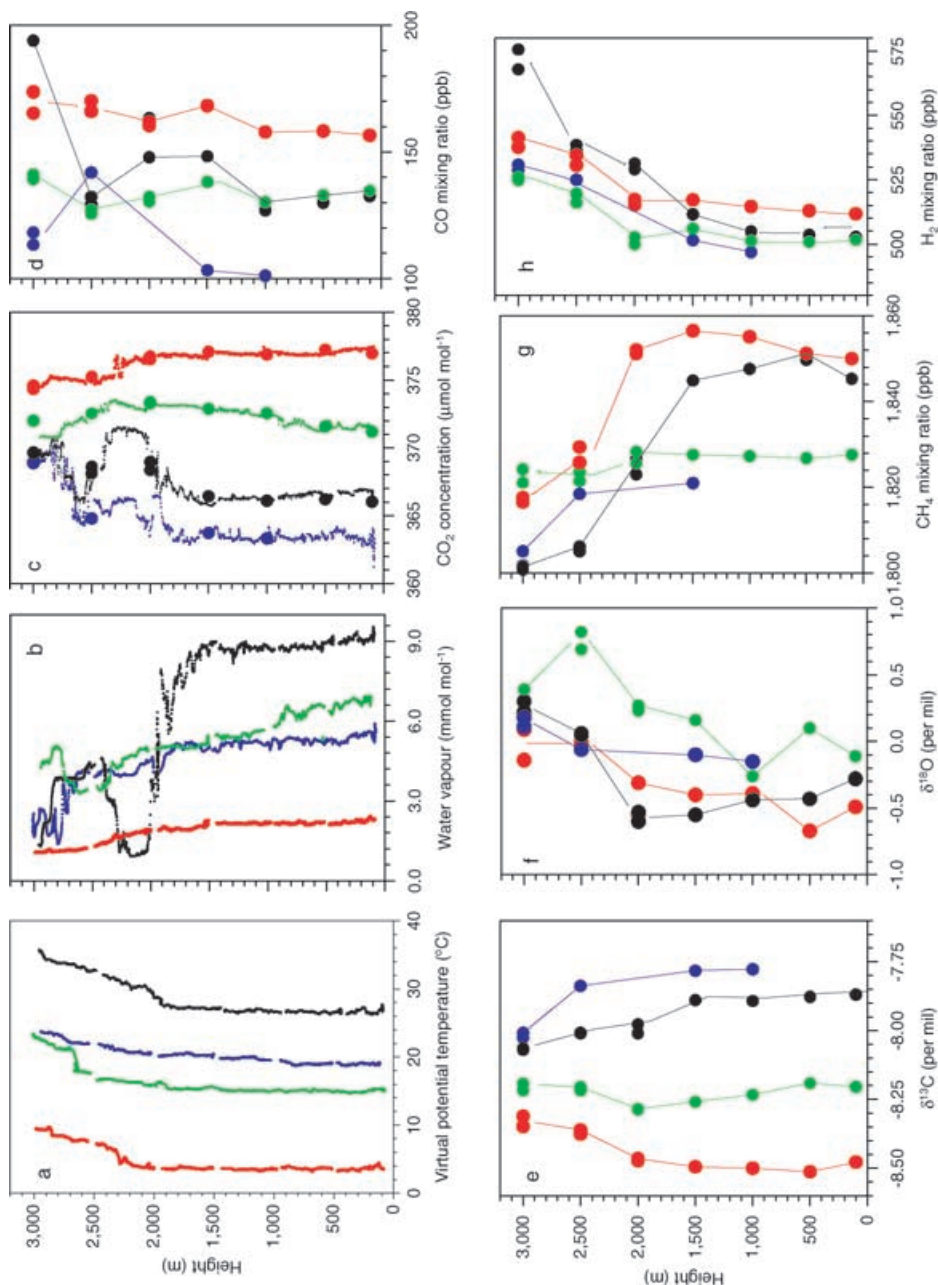


Fig. 1. Typical afternoon profiles observed during late spring and summer for (a) virtual potential temperature, (b) water vapour mole fraction, (c) CO₂ mole fraction, (d) CO mixing ratios, (e) δ¹³C of CO₂, (f) δ¹⁸O in CO₂, (g) CH₄ mixing ratios and (h) H₂ mixing ratios. For the continuous profiles in (a)–(c), red = 29 April 2000, green = 29 May 2000, black = 14 June 2000 and blue = 30 June 2000. The symbols in (c)–(f) use the same colour code and show values determined by flask sampling. Flask data at the lower levels for 30 June are not presented. The flasks involved were damaged in transit, having had an unfortunate interaction with a drunken fork-lift driver.

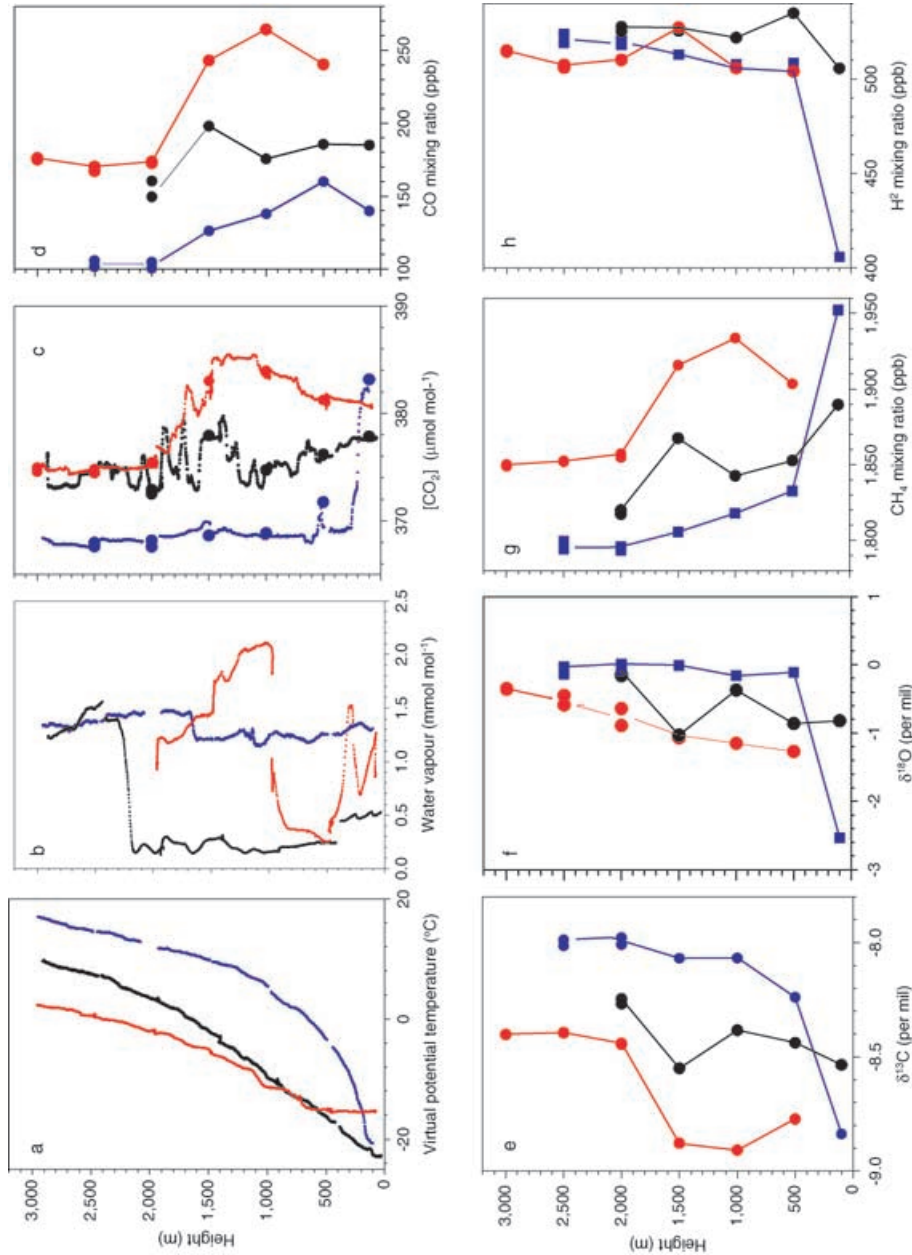


Fig. 2. Typical afternoon profiles observed during late autumn and winter for (a) virtual potential temperature, (b) water vapour mole fraction, (c) CO₂ mole fractions (d) CO mixing ratios, (e) $\delta^{13}\text{C}$ of CO₂, (f) $\delta^{18}\text{O}$ in CO₂, (g) CH₄ mixing ratios and (h) H₂ mixing ratios. For the continuous profiles in (a)–(c), blue = 28 November 1999; red = 26 January 2000, black = 4 March 2000. The symbols in (c)–(f) use the same colour code and show values determined by flask sampling.

of the CO flask measurements shows a similar pattern to the observed for CO₂. By contrast, the very high CO₂ concentrations observed at 100 m height on 28 November were not accompanied by elevated CO concentration. Nevertheless, above that height a covariance between CO₂ and CO, similar to the other two flights seen in Fig. 2 was also observed (Fig. 2d).

As for the summer flights in Fig. 1, $\delta^{13}\text{C}\text{O}_2$ profiles generally mirrored those observed for CO₂ but the pattern for $\delta^{18}\text{O}$ in CO₂ was less systematic, with values continually increasing with height above the ground for 26 January despite the irregular CO₂ profile shape. For both 22 November and 4 March the $\delta^{18}\text{O}$ in CO₂ profile was similar in form to $\delta^{13}\text{C}$, also mirroring the CO₂ profile (Fig. 2f).

As for CO, the vertical structure of CH₄ showed a similar pattern to that observed for CO₂ on 26 January and 4 March. However, in contrast to CO, the high CO₂ concentration observed at 100 m on 28 November was also accompanied by very a high CH₄ concentration, in this case 1952 ppb.

Profiles of molecular hydrogen are shown in Fig. 2h. This shows little systematic pattern to be ob-

served, either with height or in relation to the other gases examined for both 26 January and 4 March. This was not, however, the case for 28 November. Here a very low H₂ concentration of 406 ppb was observed at 100 m height, more than 100 ppb less than that measured at the next highest level of 500 m.

3.3. Relationship between CO₂, CH₄ and CO concentrations in autumn and winter

From Fig. 2 it can be seen that for both the 26 January and 4 March flights there were strong similarities in the patterns observed in the vertical structure of CO₂, CO and CH₄. In Fig. 3 the nature and frequency of such correlations are examined for all flights undertaken between 1 November and 29 March, the period for which biological activity would not be expected to be significant (Armeth et al., 2002; Shibistova et al., 2000a; Lloyd et al., 2002). Figure 3a shows the relationships between CO₂ and CO concentrations for these flights, with all values expressed relative to the lowest concentration observed for each flight. Although for some flights no clear relationship is

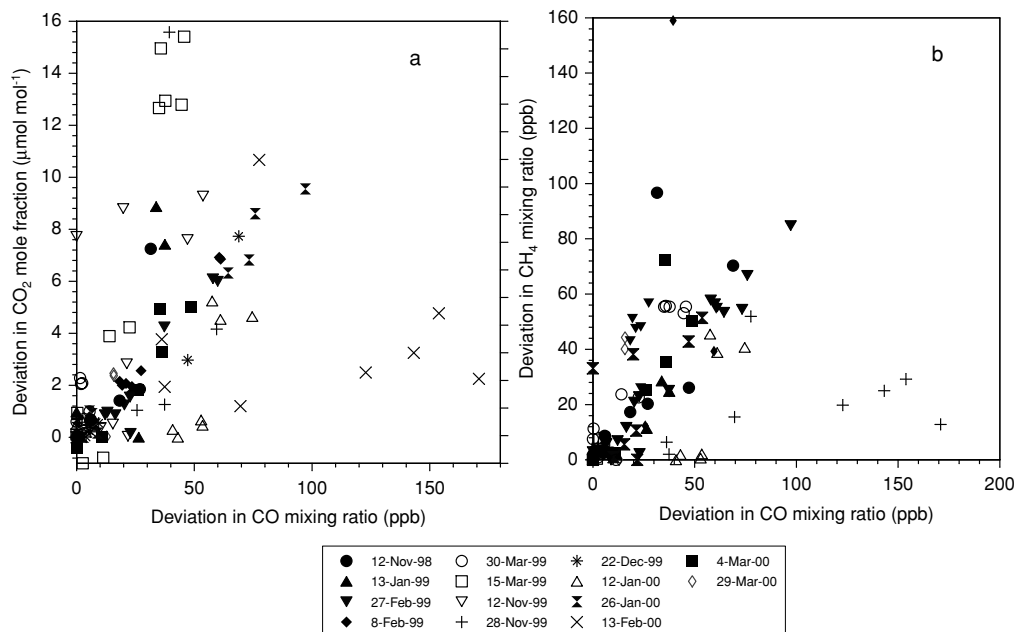


Fig. 3. Flights during the late autumn to early spring period showing the relationship between the deviation in the CO mixing ratio (expressed relative to the lowest observed value for each flight) and the corresponding deviation in (a) CO₂ mole fraction and (b) CH₄ mixing ratios.

Table 1. $\delta^{13}\text{C}$ composition of "source" CO_2 (\pm s.e.) in clean and polluted air masses during winter as determined by a plot of $\delta^{13}\text{C}$ versus $1/[\text{CO}_2]^a$

| Date | "Source" $\delta^{13}\text{C}$ (‰) | r^2 | n |
|---------------------------|------------------------------------|-------|-----|
| "Clean" flights | | | |
| 13 Jan 1999 | -27.6 ± 0.3 | 1.00 | 4 |
| 15 Mar 1999 | -27.3 ± 1.2 | 0.98 | 11 |
| 12 Nov 1999 | -27.8 ± 0.8 | 1.00 | 9 |
| 28 Nov 1999 | -29.0 ± 0.2 | 1.00 | 10 |
| "Polluted" flights | | | |
| 8 Feb 1999 | -32.0 ± 1.3 | 0.99 | 9 |
| 27 Feb 1999 | -31.4 ± 0.7 | 1.00 | 11 |
| 26 Jan 2000 | -29.8 ± 0.3 | 1.00 | 10 |
| 4 Mar 2000 | -28.9 ± 0.7 | 1.00 | 6 |

^a r^2 = correlation coefficient, n = number of observations. "Clean" versus "Polluted" air masses were determined on the basis of the $[\text{CO}_2]$ versus $[\text{CO}]$ relationship of Fig. 3a.

apparent, and this is especially the case for the three November flights, for many of the flights the relationship is strong and surprisingly consistent. For example for the flights on 8 February 1999, 27 February 1999, 26 January 2000 and 4 March 2000 the slopes of the relationship are (in $\mu\text{mol mol}^{-1} \text{CO}_2 \text{ppb}^{-1} \text{CO}$), 0.117 ± 0.007 , 0.111 ± 0.012 , 0.101 ± 0.005 and 0.128 ± 0.01 . Strong relationships were also apparent for the relationship between CH_4 and CO for many flights: for the same four flights considered above, the slopes of the relationship are (in $\text{ppb CH}_4 \text{ppb}^{-1} \text{CO}$), 0.98 ± 0.34 , 1.00 ± 0.12 , 0.86 ± 0.04 and 1.69 ± 0.50 . As is discussed below, where such strong relationships exist they are most likely indicative of the presence of polluted air masses in the sampling profile. Similarly, the lack of any relationship and the presence of a more uniform profile than that observed for 26 January and 4 March is suggestive of a relatively clean and uniform air mass. On that basis we have also selected four flights with little indications of pollution, viz. 13 Jan 1999, 15 March 1999, 12 November 1999 and 28 November 1999, and Table 1 compares the $\delta^{13}\text{C}$ of the "source" CO_2 for the two flight categories using the simple mixing model of Keeling (1961). This shows the $\delta^{13}\text{C}$ of the CO_2 associated with the "polluted" flights to be somewhere around 3‰ depleted compared to the "clean" flights.

3.4. Seasonal patterns

Boundary layer height. From a combined examination of the profiles of temperature, CO_2 concentra-

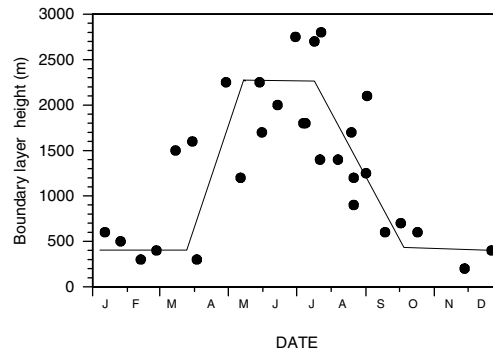


Fig. 4. Estimated afternoon boundary layer height as a function of time of year. Note that not all flights are shown here because for some flights, the height of the boundary layer could not be unequivocally determined.

tion and water vapour concentration it is often possible to detect the atmospheric boundary layer (ABL) height, and Fig. 4 shows its seasonal variability with data from all years included. Remembering that our measurements are generally made under fine weather conditions and around or after noon, ABL heights at Zotino are typically between 200 and 600 m for the period November through to February. However, as early as mid-March ABL heights of as much as 1.5 km are already observed. During the summer months the ABL can reach anywhere between 1 and 2.8 km, but the average height tends to decline gradually after early August, with minimum values again being reached around early November.

Using the ABL heights as shown in Fig. 4, one can separate each profile into an ABL and free-troposphere component. In what follows, we examine the different patterns of the seasonal cycle for the various trace gases examined for these two layers for the period 9 July 1998 to 3 November 2000.

CO_2 concentrations. The seasonal pattern in CO_2 concentrations observed in the ABL and free troposphere over the two year period examined is shown in Fig. 5a. This shows large differences in the magnitude of the seasonal cycle between the ABL and the free troposphere; the amplitude of the smoothed seasonal cycle, calculated as described by Thoning et al. (1989), is about $24 \mu\text{mol mol}^{-1}$ within the ABL and about $14 \mu\text{mol mol}^{-1}$ for the free troposphere above. Considerable variation in the CO_2 concentrations within the ABL is apparent, especially in the winter period. During the summer months CO_2 concentrations are lower in the ABL than the free troposphere,

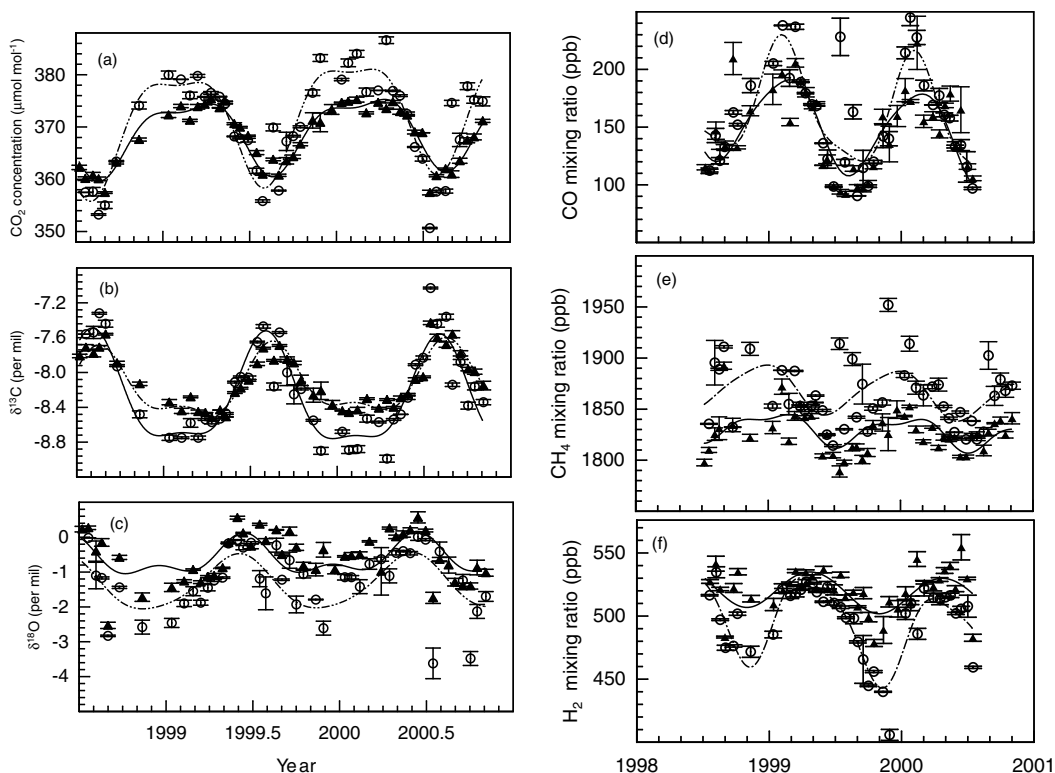


Fig. 5. (a) CO_2 mole fraction, (b) $\delta^{13}\text{C}$ in CO_2 , (c) $\delta^{18}\text{O}$ in CO_2 , (d) CO mixing ratios, (e) CH_4 mixing ratios and (f) H_2 mixing ratios within and above the boundary layer above Zotino from July 1998 to November 2000 (CO_2 , $\delta^{13}\text{C}$, $\delta^{18}\text{O}$) or from July 1998 to July 2000 (CO and H_2). Open circles, boundary layer; closed triangles; free troposphere. Standard error bars (where visible) are also shown. Most flights were done in the afternoon. The curves for boundary layer and free troposphere have been fitted as described in Thoning et al. (1989), with each point weighted according to its standard error.

whereas during the winter months the opposite is the case. The phasing of changes within the ABL precedes that in the free troposphere during both the spring draw-down and the autumn increase in the CO_2 concentrations.

$\delta^{13}\text{C}$ in CO_2 . As would be anticipated from the profiles shown in Figs. 1 and 2, the seasonal pattern on $\delta^{13}\text{CO}_2$ mirrors that of the CO_2 concentration, with a gradual depletion occurring during the autumn and winter months and enrichment occurring during spring and summer (Fig. 5b). The $\delta^{13}\text{C}$ in CO_2 is more negative in the ABL during winter, and enriched with respect to the free troposphere during spring and summer. As for the CO_2 concentration, the phasing of changes within the ABL precedes that for the free troposphere.

$\delta^{18}\text{O}$ in CO_2 . Both the free troposphere and the ABL show a depletion in the $\delta^{18}\text{O}$ in CO_2 starting in mid-

summer and an enrichment starting in early winter; a phasing that substantially lags the enrichment observed for $\delta^{13}\text{CO}_2$, or the corresponding changes in CO_2 concentration. The magnitude of the amplitude of the seasonal cycle is greater within the ABL and, unlike the $\delta^{13}\text{C}$ in CO_2 , the $\delta^{18}\text{O}$ in CO_2 is nearly always depleted in the ABL with respect to the free troposphere. In both years examined, $\delta^{18}\text{O}$ values were very similar between the free troposphere and the ABL at the seasonal cycle maximum in late April/early May. In both 1998 and especially 2000, extremely depleted values were observed in July for both the free troposphere and the ABL.

CO concentrations. These tend to be nearly always greater within the ABL than the free troposphere during the winter months, with little difference generally being observed during summer (Fig. 5d). A marked seasonal cycle is apparent for both

layers, with minimum concentrations of around 100 ppbv being observed in mid-summer, and maximum values as high as 250 ppbv occurring in late winter. Occasionally high CO is observed within the ABL in summer (for example 17 July 1999), perhaps related to the presence of forest fires in the area at that time.

CH₄ concentrations. These data were highly variable within the ABL (Fig. 5e). Nevertheless, a seasonal pattern was still discernible, with maximum values tending to be observed during winter in the free troposphere. Without exception, CH₄ concentrations were higher in the ABL than in the free troposphere with differences of as much as 100 ppbv sometimes being observed in summer and autumn.

H₂ concentrations. A distinct seasonal cycle was observed for both the free troposphere and the ABL, with minimum values being observed in late autumn and maximum concentrations occurring in early spring (Fig. 5f). Hydrogen concentrations were always lower within the ABL, especially so in summer and autumn. The example of 28 November 1999 shown in Fig. 2 is the most extreme case.

4. Discussion

As expected, a significant seasonal cycle was observed for CO₂ concentrations, both within the ABL and in the free troposphere to the maximum height of 3 km examined. The amplitude of the seasonal cycle was greater in the ABL as CO₂ concentrations were lower in summer (Fig. 1c), presumably a consequence of the marked net uptake of CO₂ by both forest and wetland vegetation in the area (Lloyd et al., 2001; Arneeth et al., 2002; Lloyd et al., 2002; Styles et al., 2002). The reasons for the higher CO₂ concentrations within the ABL during autumn, winter and early spring are less clear and most likely more complex. Although there is clear evidence for emission of CO₂ from snow-covered forest soil during winter (Shibistova et al., 2002b) as well as for a slow release of both CO₂ and CH₄ from wetlands (Panikov and Dedysh, 2000), rates are 0.1 to 0.01 of those occurring during summer and unlikely to account for the large temporal variations in CO₂, CH₄ and CO observed. Moreover, as the data in Fig. 3 show for many flights during winter, strong and consistent correlations were observed among the concentrations of these three gases. Such correlations have been observed during winter at high northern latitudes for the arctic troposphere north of Europe (Conway

et al., 1993) and also from long-term ground-based measurements during the winter dark period at Barrow, Alaska (Harris et al., 2000). In both cases the interpretation of these strong correlations has been that the variations in observed CO₂ concentrations are a consequence of variations in the amount of CO₂ attributable to industrial sources. Indeed, Harris et al. (2000) consider that most of the polluted air masses that arrive at Barrow during winter have come from Siberia. In that respect, it is interesting to note that the relationships between CO and CH₄ or CO₂ observed here are very close to those observed at Barrow for polluted air masses. Harris et al. (2000) reported a $\Delta\text{CO}_2/\Delta\text{CO}$ ratio of 0.127 ppm CO₂ ppb⁻¹ CO, rather close to the average value of 0.114 $\mu\text{mol mol}^{-1}$ CO₂ ppb⁻¹ CO as determined for "polluted flights" in the study here (Fig. 3). There are, however, some differences between the current study and Harris et al. (2000) in the $\Delta\text{CH}_4/\Delta\text{CO}$ ratios observed; these being 1.69 for polluted air masses at Barrow but only 1.13 here. An additional verification that the atmosphere sampled by at least some winter flights had been affected by polluted air masses comes from the apparent source $\delta^{13}\text{C}$ of these flights (Table 1). The source $\delta^{13}\text{C}$ as inferred from a plot of $\delta^{13}\text{C}$ versus $1/[\text{CO}_2]$ for winter flights, with strong correlations between CO₂, CH₄ and CO, was substantially depleted with respect to those that showed no such correlations. This is consistent with a depleted fossil fuel $\delta^{13}\text{C}$ source (Andres et al., 2000).

As recognized by both Conway et al. (1993) and Harris et al. (2000), the primary origin of polluted air masses detected in Alaska may actually be Europe rather than Siberia itself. This is clearly implied by our own back-trajectory analyses as well. For example, the back trajectories for the probably polluted flight of 26 January 2000 suggest that, especially at around 1600 m height, the source air had travelled from the northern part of central Europe, across the highly industrialised areas of the Baltic states and/or Poland, and then across an also heavily industrialised area of south-eastern Russia and Ukraine before entering Siberia (Fig. 6).

From Fig. 2c, we may also conclude that under the stable atmospheric conditions that tend to prevail throughout the high northern latitudes in winter (Fig. 2a) that vertical mixing is strongly suppressed and that large fluctuations in CO₂ concentrations may be observed over relatively small vertical distances. This gives rise to a dilemma in terms of evaluating "background" concentrations. A central criterion for inclusion of data into this category is that the air is

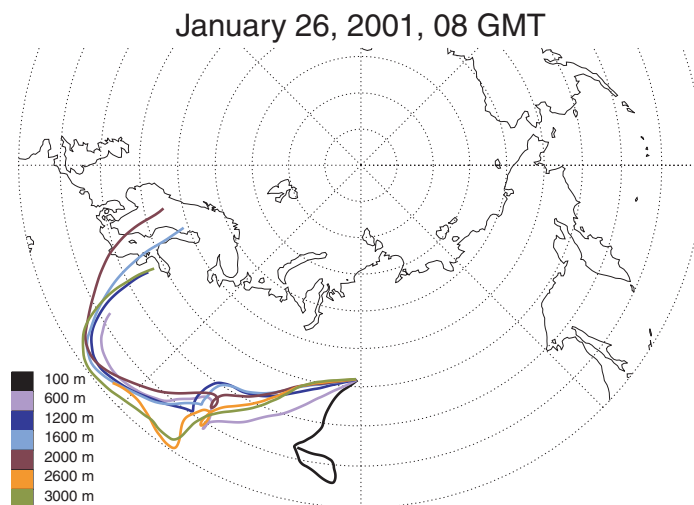


Fig. 6. Calculated 7 day back trajectories for air at 100, 600, 1200, 1600, 2000, 2600 and 3000 m heights for 26 January 2000.

well mixed. In our view, the concept of well mixed background air over Siberia for much of the winter period is not appropriate and this is probably also the case, although perhaps generally to a lesser degree, for much of the northern hemisphere. Therefore, in the simple curve fitting analysis to derive Fig. 5 we have included all data, even though it is clear from Fig. 3 that the extent to which the measured atmospheric CO_2 concentrations have been influenced by industrial sources varies from flight to flight. This approach differs from that taken by the NOAA global CO_2 monitoring network, where air masses in winter with unusually high CO_2 concentrations are automatically excluded by means of a statistical filter (Conway et al., 1994). There is a large potential impact of winter-time CO_2 concentration data selection on the estimated overall average CO_2 concentrations at the higher northern latitudes (where industrial sources are the most common), and therefore on the inferred north-to-south latitudinal gradient. This may have significant effects on the inferred magnitude of the northern-hemisphere carbon sink (Tans et al., 1990).

Although the strong correlations observed between CO_2 , CH_4 and CO concentrations and the apparent source $\delta^{13}\text{C}$ for many winter flights provides strong circumstantial evidence for the frequent presence of fossil fuel CO_2 in the Siberian atmosphere during the winter months, there were also several flights during late autumn, winter and early spring for which no such correl-

ative evidence could be found (Fig. 3). A case in point is the flight of 28 November (Fig. 2). Here a massive accumulation of CO_2 was observed within the shallow stable boundary layer, but with no corresponding elevation in CO , suggestive of a primarily biological source of CO_2 . Strong supporting evidence for this notion comes from the greatly depleted molecular hydrogen concentrations associated with the elevated CO_2 concentrations close to the ground (Fig. 2g). The major sink for H_2 is uptake by soils, which is biologically mediated and linked to the respiratory capacity of soil micro-organisms (Godde et al., 2000). Methane concentrations were also substantially elevated at 100 m. From the 7 day back trajectory analysis of Fig. 7, we can conclude that these high methane concentrations are consistent with significant biological release of this gas from the wetlands to the west of the sampling area, even in late November. Obviously significant respiratory CO_2 release and hydrogen uptake can still occur in the same region during this period as well.

As would be expected on the basis of low or negative sensible heat fluxes during the winter months (Garratt, 1992), ABL heights were generally quite low between November and early March (Fig. 4). It has been proposed that a covariance between ABL height and the seasonality of terrestrial CO_2 exchange may be one factor giving rise to the so called "rectifier effect" (Denning et al., 1995). According to this theory,

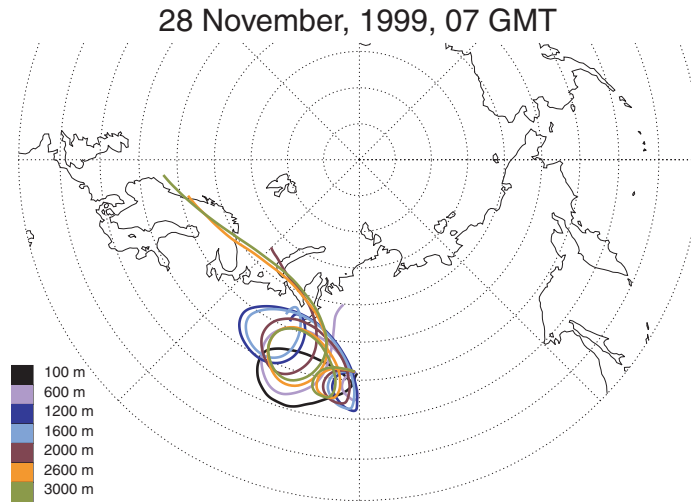


Fig. 7. Calculated 7 day back trajectories for air at 100, 600, 1200, 1600, 2000, 2600 and 3000 m heights for 28 November 1999.

mean annual CO_2 concentrations at the surface are greater than would be the case if the vertical transport of CO_2 during times of terrestrial CO_2 release (autumn through early spring) occurred at the same intensity as during summer where high ABL heights are high (Fig. 4). Cumulus convection which can mix CO_2 and other entities from the surface to high altitude is also more likely during the summer months.

Regularly obtained data of the vertical structure of atmospheric CO_2 concentrations taken over a year or more as have been obtained here, especially when considered in conjunction with ground-based CO_2 flux measurements for the same region, and at the same time (Arneeth et al., 2002; Lloyd et al., 2002) have the potential to help quantify the magnitude of this “rectifier” effect. Unfortunately, due to the likely frequent presence of polluted air masses with elevated CO_2 concentrations during winter (discussed above) it is hard to make any definitive statements as to the likely changes in CO_2 concentrations attributable to respiration only during this time and therefore the magnitude of this “rectifier” effect in central Siberia. Nevertheless, some pertinent observations can be made. Firstly, even in late January there is evidence for the occurrence of convective boundary layers, although the turbulence within such layers may not be sufficient to mix CO_2 and other entities completely (Fig. 2). By mid-March, well mixed daytime convective boundary layers (CBL) are often observed to a height of about 1.5 km (Fig. 4), mixing CO_2 from the surface to the CBL

height, much as in the profile for 29 April 2000 as is shown in Fig. 1. This CBL development and mixing of any surface fluxes in winter and in autumn can occur despite there being snow-covered ground throughout virtually all of winter and spring; this is a consequence of high radiation interception and subsequent high sensible heat fluxes from non-photosynthesising coniferous foliage when not covered by snow (Tchebakova et al., 2002).

As would be expected on the basis of the substantial discrimination against ^{13}C during photosynthetic assimilation by C_3 plants (Lloyd and Farquhar, 1994), a substantial enrichment of the $\delta^{13}\text{C}$ in CO_2 accompanied the summertime draw-down of CO_2 as observed in both the ABL and the free troposphere. Likewise, during the rapid increase in CO_2 concentrations observed in autumn, a substantial decrease in the $\delta^{13}\text{C}$ of CO_2 occurred (Fig. 5d). Nevertheless, from the analysis of the isotopic composition of “source” air during winter, it is clear that substantial differences occurred from flight to flight, with those flights considered to be affected by pollution events giving a source $\delta^{13}\text{C}$ substantially depleted compared to those where the primary source of variation was considered to be biological.

Unlike for $\delta^{13}\text{C}$, the $\delta^{18}\text{O}$ in CO_2 within the ABL were always depleted compared to the free troposphere above (Fig. 5c). A substantial enrichment in both ABL and free tropospheric values commenced around January (with little concomitant change in CO_2

concentrations) and depletion commenced in around July, perhaps subsequent to the decrease in CO₂ concentrations. The decline in early summer is most likely associated with both photosynthesis and respiration depleting the atmospheric $\delta^{18}\text{O}$ in CO₂ (Farquhar and Lloyd, 1993; Farquhar et al. 1993); this is a consequence of CO₂ in equilibrium with chloroplastic water being depleted with respect to the atmosphere at these reasonably high northern latitudes. From ground-based measurements of the relationship between the $\delta^{18}\text{O}$ of CO₂ and CO₂ concentration in early May 1999, we have determined a $\delta^{18}\text{O}$ of respired CO₂ at this time of about -25‰ (Lloyd et al., unpublished data). Vertical profiles, such as that shown for 29 May in Fig. 1, clearly suggest that associated with the daytime photosynthetic drawdown of CO₂ within the ABL is a substantial depletion of the associated $\delta^{18}\text{O}$; i.e. negative photosynthetic discrimination against oxygen-18 in CO₂. Nevertheless, CBL budgetting results also show that positive discriminations can also occur in the Zotino region during summer, at least in the afternoon periods (Styles et al., 2002).

During winter and before snowmelt in spring, rates of surface CO₂ efflux are very low in this area for both forest (Shibistova et al., 2002b) and bog (Arneeth et al., 2002) and are unlikely to impact significantly on the atmospheric $\delta^{18}\text{O}$ in CO₂ observed. Most likely then, the gradual increase in the $\delta^{18}\text{O}$ of CO₂ seen in both the ABL and free troposphere from January to April reflects mixing with air from lower latitudes that

is less depleted in $\delta^{18}\text{O}$. The continued depletion of the $\delta^{18}\text{O}$ of CO₂ in early autumn may be attributable to appreciable rates of respiration during that period (Shibistova et al., 2002a; 2002b) and with a continued depleted isotopic signature (Peylin et al., 1999). Generally speaking, the phase differences between CO₂ concentration and $\delta^{18}\text{O}$ composition observed above Zotino are similar to those observed for maritime high latitude northern sites (Trolier et al., 1996) and seems to be well explained by modelling studies (Peylin et al., 1999).

There are several noticeable “outliers” for the $\delta^{18}\text{O}$ seasonal cycle observations shown in Fig. 5c, most noticeably the extremely depleted values in both ABL and the free troposphere on 16 July 2000. We do not, however, believe that data such as this reflect measurement error, but rather may reflect the extreme heterogeneity of oxygen-18 isotopic fractionations associated with terrestrial carbon exchange in this region. For example, although the great majority of the air masses arriving at Zotino originate from the western, northerly or southern sectors (Levin et al., 2002) the 16 July 2000 air mass was unusual in that it originated from the east. In particular, for heights greater than 2000 m our trajectory analyses suggests that this air mass had passed over extensive areas of *Larix* forest and tundra (Fig. 8). Due to extreme low winter temperatures, these are areas for which the $\delta^{18}\text{O}$ of soil water would be expected to be especially depleted and appreciable negative photosynthetic discriminations against

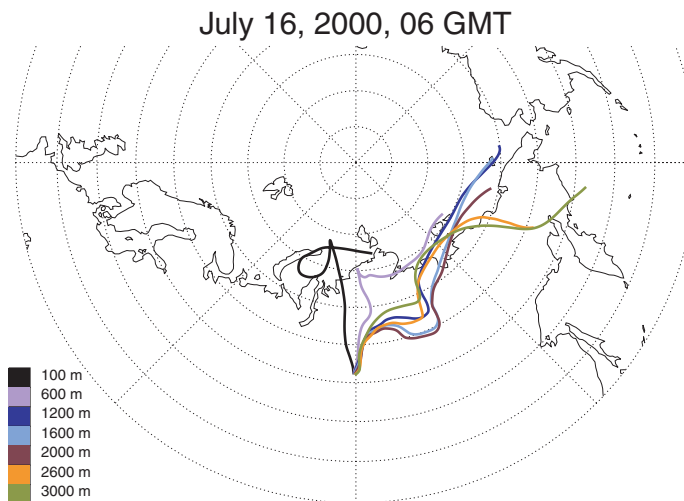


Fig. 8. Calculated 7 day back trajectories for air at 100, 600, 1200, 1600, 2000, 2600 and 3000 m heights for 16 July 2000.

$\delta^{18}\text{O}$ most likely (Farquhar et al., 1993). This is especially so given the likely reliance of permafrost forest areas on at least some water from snow-melt for their photosynthetic water supply during summer (Kelliher et al., 1997; Schulze et al., 1999; Kelliher et al. 2001). The exceptionally low CO_2 concentrations in both the free-troposphere and ABL for this flight (Fig. 5a) are also consistent with the air mass sampled having travelled extensively over photosynthetically active land areas prior to its arrival at Zotino.

Although not the prime objective of this study, ancillary measurements of CO , CH_4 and H_2 have proved valuable in the identification of CO_2 sources; in particular CO as an indicator of polluted air masses and low concentration of H_2 as a tracer for CO_2 released as a consequence of soil respiration. The seasonal patterns as shown in Figs. 5d–f also provide useful information for incorporation into global datasets.

The seasonal pattern of CH_4 was highly variable, especially in the ABL. This is probably a consequence of the measurement site being located on the eastern edge of the extensive West Siberian wetland which extends from just east of the Ural Mountains to the Yenisei River. Air masses coming from this region would be expected to have much higher CH_4 concentrations than those coming from elsewhere (Tojhma et al., 1997); a consequence of not only high CH_4 efflux rates from this large wetland area, but also probably as a consequence of venting and leakage associated with the extensive harvesting of natural gas in this region (Tojhma et al., 1996).

5. Conclusions

Forty-seven flights sampling the atmosphere to a height of 3000 m have been undertaken near Zotino in central Siberia between July 1998 and November 2000. The data show the amplitude of the seasonal cycle in CO_2 concentrations in the free troposphere to be about $14 \mu\text{mol mol}^{-1}$ and with atmospheric boundary layer to be about $24 \mu\text{mol mol}^{-1}$. Boundary-layer

heights vary from 200–600 m in winter to as much as 2800 m in summer.

The vertical structure of CO_2 concentration is often complex in winter, and concurrent variations in $\delta^{13}\text{CO}_2$, and CO and CH_4 mixing ratios suggest that this may be due varying amounts of polluted air being present. Trajectory analyses suggest the primary origin of these polluted air masses somewhere in Europe.

The vertical structure of the oxygen isotopic composition of CO_2 shows its $\delta^{18}\text{O}$ to almost always be more depleted in the ABL than in the free troposphere above, irrespective of the shape of the CO_2 concentration profile. We interpret this as indicating a net negative discrimination being associated with the net terrestrial carbon exchange, irrespective of whether photosynthesis or respiration dominates the net carbon flux in this region.

Marked seasonal variations in CO and H_2 are also observed above central Siberia, but seasonal patterns CH_4 mixing ratios are less distinct, presumably due the large-scale heterogeneity of wetlands in the source region. Throughout the year, CH_4 mixing ratios are consistently higher within the ABL than the free troposphere above, whereas the opposite is the case for H_2 mixing ratios, especially during late autumn. The occasional covariations in H_2 and CO_2 concentrations for unpolluted air masses during autumn suggest that H_2 may in some cases be useful as a tracer for atmospheric CO_2 with a recent origin from soil respiratory activity.

6. Acknowledgements

We thank Olaf Kolle and Karl Kubler for construction of the continuous profiling system and the many people who helped with the airborne flask sampling at one time or another: Julie Styles, Kieran Lawton, Johannes Laubach, Andrej Sogachev, Almut Arneith and Martin Heimann. We also thank Lisa Cooper for analyses and data processing in GASLAB.

REFERENCES

- Allison, C. E. and Francey, R. J. 1999. $\delta^{13}\text{C}$ of atmospheric CO_2 at Cape Grim: The in-situ record, the flask record, air standards and the CG92 calibration scale. In: *Baseline Atmospheric Program (Australia) 1996* (eds. ??Gras, J. N., Tindale and N. Derek). Bureau of Meteorology and CSIRO Division of Atmospheric Research, Melbourne Australia, 45–56.
- Andres, R. J., Marland, G., Boden, T. and Bischof, S. 2000. Carbon dioxide emissions from fossil fuel consumption and cement manufacture 1751–1991; and an estimate of their isotopic composition and latitudinal distribution. In: *The carbon cycle* (eds. T. Wigley and D. Schimel). Cambridge University Press, Cambridge, 53–62.

- Arneth, A., Kurbatova, J., Kolle, O., Shibistova, O., Lloyd, J., Vygodskaya, N. N. and Schulze, E.-D. 2002. Comparative ecosystem-atmosphere exchange of energy and mass in a European Russian and a central Siberian bog II. Inter-seasonal and interannual variability of CO₂ fluxes. *Tellus* **54B**, this issue.
- Ciais, P., Tans, P. P., White, J. W. C., Trolier, M., Francey, R. J., Berry, J. A., Randall, D., Sellers, P., Collatz, J. G. and Schimel, D. S. 1995. Partitioning of ocean and land uptake of CO₂ as inferred by $\delta^{13}\text{C}$ measurements from the NOAA Climate Modelling and Diagnostics Laboratory Global Air Sampling Network. *J. Geophys. Res.* **100**, 5051–5070.
- Ciais, P., Peylin, P. and Bousquet, P. 2000. Regional biospheric carbon fluxes as inferred from atmospheric CO₂ measurements. *Ecol. Appl.* **10**, 1574–1589.
- Conway, T. J., Steele, L. P. and Novelli, P. C. 1993. Correlations among atmospheric CO₂, CH₄ and CO in the arctic, March 1989. *Atmos. Environ.* **27A**, 2881–2894.
- Conway, T. J., Tans, P. P., Waterman, L. S., Thoning, K. A., Kitzis, D. R., Masarie, K. A. and Zhang, N. 1994. Evidence for interannual variability of the carbon cycle from the NOAA/CMDL global air sampling network. *J. Geophys. Res.* **99**, 22831–22855.
- Crutzen, P. J., 1991. Atmospheric chemistry–Methane sinks and sources. *Nature* **350**, 380–381.
- Crutzen, P. and Andreae, M. O. 1990. Biomass burning in the tropics–Impact on atmospheric chemistry and biogeochemical cycles. *Science* **250**, 1669–1678.
- Denning, A. C., Fung, I. Y. and Randall, D. 1995. Latitudinal gradient of atmospheric CO₂ due to seasonal exchange with land biota. *Nature* **376**, 240–243.
- Draxler, R. and Hess, G. D. 1998. An overview of the HYSPLIT modelling system for trajectories, dispersion and deposition. *Aust. Meteorol. Mag.* **47**, 295–308.
- Enting, I. G., 1993. Inverse problems in atmospheric constituent studies. *Inverse Problems* **9**, 649–665.
- Fan, S., Gloor, M., Mahlman, J., Pacala, S., Sarmiento, J., Takahashi, T. and Tans, P. 1999. A large terrestrial sink in North America implied by atmospheric and oceanic carbon dioxide data and models. *Science* **282**, 754–759.
- Farquhar, G. D. and Lloyd, J. 1993. Carbon and oxygen isotope effects in the exchange of carbon dioxide between terrestrial plants and the atmosphere. In: *Stable isotopes in plant water relations* (eds. J. A., Ehleringer, A. E., Hall and G. D., Farquhar). Academic Press, San Diego, 47–70.
- Farquhar, G. D., Lloyd, J., Taylor, J. A., Flanagan, L. B., Syvertsen, J. P., Hubick, K. T., Wong, S. C. and Ehleringer, J. A. 1993. Vegetation effects on the oxygen isotopic composition of atmospheric CO₂. *Nature* **363**, 439–443, 1993.
- Francey, R. J. and Tans, P. P. 1987. Latitudinal variation in oxygen-18 of atmospheric CO₂. *Nature* **337**, 496–497.
- Francey, R. J., Steele, L. P., Langenfelds, R. L., Lucarelli, M. P., Allison, C. E., Beardsmore, D. J., Coram, S. A., Derek, N., de Silva, F., Etheridge, D. M., Fraser, P. J., Henry, R., Turner, B. and Welch, E. D. 1996. Global Atmospheric Sampling Laboratory (GASLAB): supporting and extending the Cape Grim trace gas programs. In: *Baseline Atmospheric Program (Australia) 1993* (eds. R. J. Francey, A. L., Dick and N., Derek). Bureau of Meteorology and CSIRO Division of Atmospheric Research: Melbourne, 8–29.
- Fung, I. Y., Prentice, K., Matthews, E., Lerner, J. and Russell, G. 1983. Three-dimensional tracer model study of atmospheric CO₂: response to seasonal exchanges with the terrestrial biosphere. *J. Geophys. Res.* **88**, 1281–1294.
- Garratt, J. R., 1992. *The Atmospheric Boundary Layer*. Cambridge University Press, Cambridge.
- Gloor, M., Fan, S.-M., Pacala, S. W. and Sarmiento, J. L. 2000. Optimal sampling of the atmosphere for purpose of inverse modelling: A model study. *Global Biogeochem. Cycles* **14**, 407–428.
- Gloor, M., Bakwin, P., Hurst, D., Lock, L., Draxler, R. and Tans, P., 2001. What is the footprint of a tall tower? *J. Geophys. Res.* **106**, 17831–17840.
- Godde, R., Meuser, K. and Conrad, R. 2000. Hydrogen consumption and carbon monoxide production in soils with different properties. *Biol. Fert. Soil* **32**, 129–134.
- Grace, J., Lloyd, J., Macintyre, J. A., Miranda, A. C., Meir, P., Miranda, H. S., Nobre, C. A., Moncrieff, J., Massheder, J., Wright, I. R. and Gash, J. H. C., 1995. Carbon dioxide uptake by undisturbed tropical rainforest, 1992 and 1993. *Science* **270**, 778–780.
- Harris, J. M., Dlugokencky, E. J., Oltmans, S. J., Tans, P. P., Conway, T. J., Novelli, P. C., Thoning, K. W. and Kahl, J. D. W. 2000. An interpretation of trace gas correlations during Barrow, Alaska, winter dark periods, 1986–1997. *J. Geophys. Res.* **105**, 17267–17278.
- Jordan, A. and Brand, W. A. 2001. Trace gas measurement and quality assurance at the MPI for Biogeochemistry, *Report to the 11th WMO/IAEA Meeting of Experts on CO₂ and related tracer measurement techniques, Tokyo, Sep. 2001*. Annex B6 (Germany) 38–42.
- Kaminski, T., Heimann, M. and Giering, R. 1999. A coarse grid three-dimensional global inverse model of the atmospheric transport–2. Inversion of the transport of CO₂ in the 1980s. *J. Geophys. Res.* **104**, 18555–18581.
- Keeling, C. D., 1961. The concentrations and isotopic abundances of atmospheric carbon dioxide in rural and marine air. *Geochem Cosmochim. Acta* **24**, 277–298.
- Kelliher, F. M., Hollinger, D. Y., Schulze, E.-D., Vygodskaya, N. N., A., Byers, J. N., Hunt, J. E., McSeveny, T. M., Milukova, I. M., Sogatchev, A., Varlagin, A., Ziegler, W., Arneth, A., Bauer, G. 1997. Evaporation from an eastern Siberian larch forest. *Agric. For. Meteorol.* **85**, 135–147.
- Kelliher, F. M., Lloyd, J., Baldocchi, D. D., Rebmann, C., Wirth, C. and Schulze, E.-D. 2001. Evaporation in the boreal zone: Physics, vegetation and climate. In: *Global biogeochemical cycles in the climate system* (eds. E. D., Schulze, S. P., Harrison, M., Heimann, E. A., Holland, J., Lloyd, I. C., Prentice and D. Schimel). Academic Press, New York, 151–175.
- Langenfelds, R. L., Steele, L. P., Allison C. E., and Francey R. J., 2001. GASLAB Calibration Information. Internal Report, CSIRO Atmospheric Research, Aspendale,

- Australia (available at www.dar.csiro.au/res/gac; version release date 19-Apr-2001).
- Law, R. M., Rayner, P. J., Denning, A. S., Erickson, D., Heimann, M., Piper, S. C., Ramonet, M., Taguchi, S., Taylor, J. A., Trudinger, C. M. and Watterson, I. G. 1996. Variations in modeled atmospheric transport of carbon dioxide and the consequences for CO₂ inversions. *Global Biogeochem. Cycles* **10**, 783–796.
- Levin, I., Ciais, P., Langenfelds, R. L., Schmidt, M., Ramonet, M., Siderov, K., Tchebakova, N. M., Gloor, M., Heimann, M., Schulze, E. D., Vygodskaya, N. N., Shibistova, O. and Lloyd, J. 2002. Three years of trace gas observations over the EuroSiberian domain derived from aircraft sampling – a concerted action. *Tellus* **54B**, this issue.
- Lloyd, J., 1999. Current perspectives on the terrestrial carbon cycle. *Tellus* **51B**, 336–342.
- Lloyd, J. and Farquhar, G. D. 1994. ¹³C discrimination during photosynthetic assimilation by the terrestrial biosphere. *Oecology* **99**, 201–215.
- Lloyd, J., Francey, R. J., Sogachev, A., Byers, J. N., Mollicone, Raupach, M. R., Kelliher, F. M., Arneth, A., Rebmann, C., Valentini, R. S., Wong, S.-C. and Schulze, E.-D., 2001. Vertical profiles, boundary layer budgets and regional flux estimates for CO₂, its ¹³C/¹²C ratio, and for water vapour above a forest/bog mosaic in central Siberia. *Global Biogeochem. Cycles* **15**, 267–284.
- Lloyd, J., Shibistova, O., Zolotoukhine, D., Kolle, O., Arneth, A., Styles, J., Tchebakova, N. M. and Schulze, E.-D. 2002. Seasonal and annual variations in the photosynthetic productivity and carbon balance of a central Siberian pine forest. *Tellus* **54B**, this issue.
- Masarie, K. A., Langenfelds, R. L., Allison, C. E., Conway, T. J., Dlugokencky, E. J., Francey, R. J., Novelli, P. C., Steele, L. P., Tans, P. P., Vaughn, B., White J. W. C. and Trolrier, M., 2001. The NOAA/CSIRO Flask-Air Intercomparison Program: A strategy for directly assessing consistency among atmospheric measurements derived by independent laboratories. *J. Geophys. Res.* **106**, 20445–20464.
- Nakazawa, T., Sugawara, S., Inoue, G., Machida, T., Maksyutov, S. and Mukai, H. 1997. Aircraft measurements of the concentrations of CO₂, CH₄, N₂O and CO and the carbon and oxygen isotopic ratios of CO₂ in the troposphere over Russia. *J. Geophys. Res.* **102**, 3843–3859.
- Novelli, P. C., Land, P. M., Masarie, K. A., Hurst, D. F., Myers, R. and Elkins, J. W. 1999. Molecular hydrogen in the troposphere: Global distribution and budget. *J. Geophys. Res.* **104**, 30427–30444.
- Panikov, N. S. and Dedysh, S. N. 2000. Cold season CH₄ and CO₂ emissions from boreal peat bogs (West Siberia): Winter fluxes and thaw activation dynamics. *Global Biogeochem. Cycles* **14**, 1071–1080.
- Peylin, P., Ciais, P., Denning, A. S., Tans, P. P., Berry, J. A. and White, J. W. C. 1999. A 3-dimensional study of δ¹⁸O in atmospheric CO₂: contribution of different land ecosystems. *Tellus* **51**, 642–667.
- Phillips, O. L., Malhi, Y., Higuchi, N., Laurance, W. F., Núñez, V., Vásquez, M., Laurance, S. G., Ferreira, L. V., Stern, M., Brown, S. and Grace, J. 1998. Changes in the carbon balance of tropical forests: Evidence from long-term plots. *Science* **282**, 439–442.
- Ramonet, M., Ciais, P., Nepomniachii, I., Siderov, K., Neubert, R., Picard, D., Kazan, V., Biraud, S., Kolle, O., Schulze, E.-D. and Lloyd, J. 2002. Three years of aircraft CO₂ and isotope measurements over Fyodorovskoye in European Russia. *Tellus* **54B**, this issue.
- Rayner, P. J. and Law, R. M. 1995. A comparison of modelled responses to prescribed CO₂ sources. CSIRO Division of Atmospheric Research Technical Paper No. 36.
- Rayner, P. J., Enting, I. G., Francey, R. J. and Langenfelds, R. 1999. Reconstructing the recent carbon cycle from atmospheric CO₂, δ¹³C and O₂/N₂ observations. *Tellus* **51B**, 213–232.
- Schulze, E.-D., Vygodskaya, N. N., Tchebakova, N., Czimczik, C. I., Kozlov, D., Lloyd, J., Mollicone, D., Myachkova, E., Sidorov, K., Varlagin, A. and Wirth, C. 2002. The EuroSiberian transect: An introduction to the experimental region. *Tellus* **54B**, this issue.
- Shibistova, O., Lloyd, J., Zrazhevskaya, G., Arneth, A., Kolle, O., Knohl, A., Astrakhantcheva, N., Shijneva, I. and Schmerler, J. 2002a. Annual ecosystem respiration budget for a *Pinus sylvestris* stand in central Siberia. *Tellus* **54B**, this issue.
- Shibistova, O., Lloyd, J., Evgrafova, S., Savushkina, N., Zrazhevskaya, G., Arneth, A., Knohl, A., Kolle, O. and Schulze, E.-D. 2002b. Seasonal and spatial variability in soil CO₂ efflux rates for a central Siberian *Pinus sylvestris* forest. *Tellus* **54B**, this issue.
- Styles, J., Lloyd, J., Zolotoukhine, D., Lawton, K. A., Tchebakova, N. M., Francey, R. J., Arneth, A., Kolle, O. and Schulze, E.-D. 2002. Estimates of regional surface carbon and oxygen isotopic discrimination, profiles of CO₂ concentration and its isotopic composition in the convective boundary layer. *Tellus* **54B**, this issue.
- Tans, P. P., Fung, I. Y. and Takahashi, T. 1990. Observational constraints of the global atmospheric CO₂ budget. *Science* **247**, 1431–1438.
- Tans, P. P., Bakwin, P. S. and Guenther, D. W. 1996. A feasible global carbon observing system: A plan to decipher today's carbon cycle based on observations. *Global Change Biol.* **2**, 309–318.
- Tchebakova, N., Kolle, O., Zolotoukhine, D., Arneth, A., Styles, J., Vygodskaya, N., Schulze, E.-D., Shibistova, O. and Lloyd, J. 2002. Inter-annual and seasonal variations of energy and water vapour fluxes above a *Pinus sylvestris* forest in the Siberian middle taiga. *Tellus* **54B**, this issue.
- Thoning, K. W., Tans, P. P. and Komhyr, W. D. 1989. Atmospheric carbon dioxide at Mauna Loa observatory 2. Analysis of the NOAA GMCC data, 1974–1985. *J. Geophys. Res.* **94**, 8549–8565.
- Tohjima, Y., Wakita, H., Maksyutov, S., Machida, T., Inoue, G., Vinnichenko, N. and Khattatov, V. 1997. Distribution of tropospheric methane over Siberia in July 1993. *J. Geophys. Res.* **102**, 25371–25382.

- Trolier, M., White, J. W. C., Tans, P. P., Masarie, K. A. and Gemery, P. A. 1996. Monitoring the isotopic composition of atmospheric CO₂: Measurements from the NOAA global air sampling network. *J. Geophys. Res.* **101**, 25897–25916.
- Werner, R. A. and Brand, W. A. 2001. Referencing strategies and techniques in stable isotope ratio analysis. *Rapid Commun. Mass Spectrom.* **15**, 501–519.
- Werner, R. A., Rothe M. and Brand W. A. 2001. Extraction of CO₂ from air samples for isotopic analysis and limits to ultra high precision $\delta^{18}\text{O}$ determination in CO₂ gas. *Rapid Commun. Mass Spectrom.* **15**, 2152–2167.
- Wirth, C., Schulze, E.-D., Schulze, W., von Stünzer-Karbe, W., Zeigler, W., Milyukova, I. M., Sogatchev, A., Varlagin, A. B., Panfyorov, M., Grigoriev, S., Kusnetova, V., Siry, M., Hards, G., Zimmermann, R. and Vygodskoya, N. N. 1999. Above-ground biomass and structure of pristine Siberian Scots pine forests as controlled by competition and fire. *Oecology* **121**, 66–80.